

# Generation of single-charge optical vortices with an uniaxial crystal

Alexander Volyar<sup>1,2</sup>, Vladlen Shvedov<sup>1,2</sup>, Tatyana Fadeyeva<sup>2</sup>,  
Anton S. Desyatnikov<sup>1</sup>, Dragomir N. Neshev<sup>1</sup>, Wieslaw Krolikowski<sup>1</sup>,  
and Yuri S. Kivshar<sup>1</sup>

<sup>1</sup>*Nonlinear Physics Center and Laser Physics Center, Research School of Physical Sciences and Engineering, Australian National University, Canberra ACT 0200, Australia*

<sup>2</sup>*Department of Physics, Taurida National University, Simferopol 95007 Crimea, Ukraine*  
[asd124@rsphysse.anu.edu.au](mailto:asd124@rsphysse.anu.edu.au)

<http://www.rsphysse.anu.edu.au/nonlinear>

**Abstract:** We implement a novel experimental technique for generating mono- and polychromatic optical beams with on-axis single vortex by manipulating polarization singularities of light in birefringent crystals. We demonstrate that, in contrast to the well-known optical quadrupoles generated by beams propagating along the optical axis of a uniaxial crystal, the beam bearing isolated single-charge on-axis vortex can be generated if the incident beam is tilted with respect to the optical axis at a certain angle.

© 2006 Optical Society of America

**OCIS codes:** (030.1640) Coherence; (030.1670) Coherent optical effects; (350.5030) Phase

---

## References and links

1. J.F. Nye and M.V. Berry, "Dislocations in wave trains," *Proc. R. Soc. London A* **336**, 165–190 (1974).
2. M. S. Soskin and M. V. Vasnetsov, "Singular optics," in *Progress in Optics*, Vol. 42, Ed. E. Wolf (North-Holland, Amsterdam, 2001), p.p. 219-276.
3. *Optical Vortices*, Eds. M. Vasnetsov and K. Staliunas, Vol. 228 of Horizons in World Physics (Nova Science, Huntington, N.Y., 1999).
4. See an extensive list of references on optical vortices in G. A. Swartzlander, Jr., Singular Optics/Optical Vortex References, <http://www.u.arizona.edu/~grovers/SO/so.html>.
5. V. Yu. Bazhenov, M. V. Vasnetsov, and M. S. Soskin, "Laser beams with screw dislocations in their wavefronts," *JETP Lett.* **52**, 429–431 (1990).
6. N. R. Heckenberg, R. McDuff, C. P. Smith, and A. G. White, "Generation of optical phase singularities by computer-generated holograms," *Opt. Lett.* **17**, 221–223 (1992).
7. A. S. Desyatnikov, Yu. S. Kivshar, and L. Torner, "Optical vortices and vortex solitons," in *Progress in Optics*, Vol. 47, Ed. E. Wolf (North-Holland, Amsterdam, 2005), p.p. 291-391.
8. See, e.g., J. Leach and M. J. Padgett, "Observation of chromatic effects near a white-light vortex," *New J. Phys.* **5**, 154.1-154.7 (2003), and references therein.
9. I. V. Basistiy, V. Yu. Bazhenov, M. S. Soskin, and M. V. Vasnetsov, "Optics of light beams with screw dislocations," *Opt. Commun.* **103**, 422–428 (1993).
10. M. V. Berry and M. R. Dennis, "The optical singularities of birefringent dichroic crystals," *Proc. R. Soc. London A* **459**, 1261–1292 (2003).
11. M. V. Berry "Conical diffraction asymptotics: fine structure of Poggendorff rings and axial spike," *J. Opt. A* **6**, 289–300 (2004).
12. M. S. Soskin and M. V. Vasnetsov, "Nonlinear singular optics," *Pure Appl. Opt.* **7**, 301–311 (1998).
13. J. F. Nye, *Natural Focusing and Fine Structure of Light*, IOP Publishing (Bristol and Philadelphia, 1999), p. 327.
14. A. V. Volyar and T. A. Fadeyeva, "Generation of singular beams in uniaxial crystals," *Opt. Spectrosc.* **94**, 235–244 (2003).
15. F. Flossmann, U.T. Schwarz, M. Maier, and M.R. Dennis, "Polarization singularities from unfolding an optical vortex through a birefringent crystal," *Phys. Rev. Lett.* **95**, 253901 (2005).

16. V. Shvedov, W. Krolikowski, A. Volyar, D. N. Neshev, A. S. Desyatnikov and Yu. S. Kivshar, "Focusing and coherence properties of white-light optical vortices," *Opt. Express* **13**, 7393–7398 (2005).
17. N. N. Rosanov, "Propagation of laser radiation in anisotropic media," *Opt. Spectrosc.* **93**, 746–741 (2002).
18. A. V. Volyar and T. A. Fadeyeva, "Laguerre-Gaussian beams in uniaxial crystals," *Ukr. J. Phys. Opt.* **5**, 81–86 (2004).
19. O. Angelsky, A. Mokhun, I. Mokhun, and M. Soskin, "The relationship between topological characteristics of component vortices and polarization singularities," *Opt. Commun.* **207**, 57–65 (2002).
20. M. R. Dennis, "Polarization singularities in paraxial vector fields: morphology and statistics," *Opt. Commun.* **213**, 201–221 (2002).
21. Yu. A. Egorov, T. A. Fadeyeva, and A. V. Volyar, "Fine structure of singular beams in crystals: colours and polarization," *J. Opt. A* **6**, S217–S228 (2004).
22. A. V. Volyar and T. A. Fadeyeva, "Dynamics of topological multiples: 2. Birth, annihilation and evolution of nonparaxial optical vortices," *Opt. Spectrosc.* **92**, 253–262 (2002).
23. O. V. Angelsky, I. I. Mokhun, and M. S. Soskin, "Interferometric methods in diagnostics of polarization singularities," *Phys. Rev. E* **65**, 036602 (2002).
24. M. S. Soskin, P. V. Polyansky, and O. O. Arkheluyk, "Computer-synthesized hologram-based rainbow vortices," *New J. Phys.* **6**, 196 (2004).
25. M. Berry, "Coloured phase singularities," *New J. Phys.* **4**, 66 (2002).

## 1. Introduction

The fundamental properties of wave dislocations [1] receive a growing attention due to a rapid experimental progress in generating various singular optical beams as well as their many promising applications [2, 3, 4]. A number of different techniques for generating optical vortices have been realized, among which the use of computer-generated holograms [5] and spiral phase plates [6] have found the widest application. However, these methods often limit both the efficiency and quality of generated optical vortices, and these issues become particularly important for vortices in nonlinear media [7] as well as for singular beams created by broad-spectrum femtosecond pulses or partially coherent and polychromatic light [8].

New exciting opportunities of the singular optics are found in the use of anisotropic optical crystals [9, 10, 11, 12]. Because of topological properties of the polarization singularities [13], which appear when the light beam strongly diffracts in a birefringent crystal, a stable generation of singular beams of a complex structure, topological multipoles, is possible from a Gaussian beam [14]. Additionally, the propagation of an initially scalar vortex in a birefringent crystal leads to the so-called vortex unfolding into different types of polarization singularities [15]. While topological multipoles consist of several spatially separated vortices, the double-charge vortex beam can be generated from a circularly polarized Gaussian beam [16].

In this paper, we suggest and implement a novel method for generating single-charge optical vortices. We study the propagation of initially linearly polarized beam in an uniaxial crystal and subsequent formation of a topological quadrupole, i.e. the structure of four vortices with alternating unit charges. We demonstrate that single-charge vortices can be generated if the beam is tilted in a specific direction with respect to the crystal axis. This technique allows also for generation of white-light vortex beams without any additional modifications.

## 2. Topological quadrupole: theory vs. experiment

We consider the propagation of a light beam along the optical axis  $z > 0$  of a homogeneous crystal described by a dielectric permeability tensor in the form  $\hat{\epsilon} = \text{diag}(\epsilon_{ij})$ , where  $\epsilon_{11} = \epsilon_{22} = \epsilon$  and  $\epsilon_{33} = \epsilon_3$ . In the paraxial approximation, the evolution of a slowly varying envelope of the transverse electric field  $\mathbf{E}(x, y, z) = \{E_x, E_y\}$  is governed by the vectorial equation [17, 18]:

$$\nabla_{\perp}^2 \mathbf{E} + 2ik\sqrt{\epsilon}\partial_z \mathbf{E} = \alpha \nabla_{\perp} (\nabla_{\perp} \mathbf{E}), \quad (1)$$

where  $\alpha = \Delta\epsilon/\epsilon_3$  and  $\Delta\epsilon = \epsilon_3 - \epsilon$ . For beams propagating along the optical axis, these equations can be solved analytically [14], however small deviations from the on-axis propaga-

tion significantly complicates the problem. Therefore, we solve Eq. (1) numerically using the pseudo-spectral method and fast Fourier transform.

We consider the propagation of a Gaussian beam with the  $x$ -linear polarization at the input ( $z = 0$ ). During its propagation in the crystal, the beam becomes elliptically polarized ( $y$ -polarized component appears), as follows from Eq. (1). The beam total intensity preserves its Gaussian shape while the intensities of  $x$ - and  $y$ - polarization components of the beam undergo a drastic change. Figures 1(a,b) illustrate the intensity and phase of the  $x$ -polarized component at the output facet of the crystal. We observe four characteristic intensity zeros which appear symmetrically on the ring surrounding the beam origin. One of these zeros from the right top quarter is also depicted in Fig. 1(b) by the contour lines with the background colors proportional to the values of the phase, from  $-\pi$  (blue) to  $\pi$  (red). The clockwise growth of the phase by  $2\pi$  indicates the presence of a vortex with the topological charge  $-1$ . The four vortices in Fig. 1(a) have alternating topological charges and they form a *topological quadrupole*.

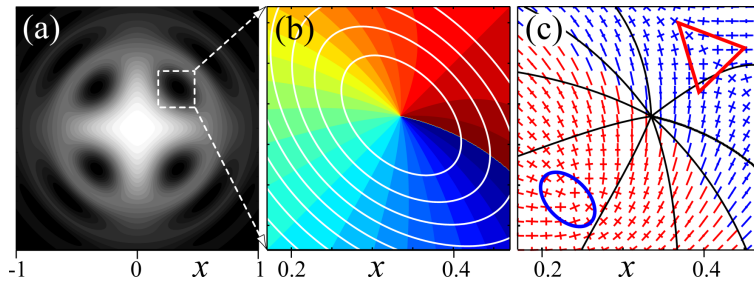


Fig. 1. Numerically calculated (a) intensity and (b) phase profiles of the  $x$ -polarized field component  $E_x(x, y, l)$  from Eq. (1) with  $\alpha = 0.07$ ;  $l \approx 6$  mm is the crystal length. The movie (**quadrupol, 1.1MB**) demonstrates the formation of a topological quadrupole in (a) during beam propagation. (c) The polarization map of the total transmitted field  $\mathbf{E}(x, y, l)$  with ellipses of the left-hand (red) and right-hand (blue) polarizations indicated by their main axes. Blue ellipse and red triangle indicate the ‘monster’ and ‘star’ polarization singularities.

To uncover the physical origin of the phase singularities which appear during the propagation of an initially smooth  $x$ -polarized beam, in Fig. 1(c) we present a map of the polarization states of the total field in the vicinity of the vortex core from Fig. 1(b). The polarization ellipses with different handedness cover most of the area (red and blue regions) while polarization became linear on the so-called  $L$ -line between these regions. There are two isolated singular points in Fig. 1(c), the  $C$ -points, where the field is circularly polarized. These points are enclosed by peculiar patterns [13, 19] indicated by ellipse and triangle in Fig. 1(c). Using analytical results for the field distributions [14] and the method to determine the positions and the types of  $C$ -points developed by M. Dennis [20], we identify our  $C$ -points as the ‘monster’- and the ‘star’-type polarization dislocations, respectively.  $C$ -points are associated with optical vortices because one of the circularly polarized components vanishes while its phase is undefined. Such vortices can be selected from a vector field by a polarization filter which can suppress either the right-hand or the left-hand circular polarization [16, 21].

If we connect two neighboring  $C$ -points of the star and monster by a straight line in Fig. 1(c), this line will cross the  $L$ -line at the point with the  $y$ -polarization, an isolated point where the  $x$ -polarized component vanishes. The phase of the  $x$ -component is shown in Fig. 1(c) by the contour lines forming the characteristic “spider” pattern with uncertainty at the central point. If we select the singular  $E_x$  component of the field with a polarizer placed behind the crystal, we will effectively convert the polarization singularity into an optical vortex. Thus, only a polarizer is sufficient to select four optical vortices composed into a topological quadrupole [14, 22].

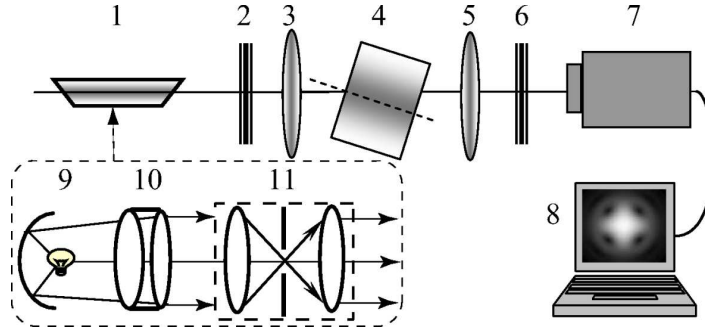


Fig. 2. Experimental setup: laser 1; polarizers 2,6; lenses 3,5; sapphire crystal 4; CCD camera 7; computer 8; white-light source 9; collimator 10; pinhole filter 11.

To prove our theoretical predictions experimentally, we employ the setup shown in Fig. 2. The beam from a cw laser 1 ( $\lambda = 532$  nm) passes through a polarizer 2 and is focused by a lens 3 into a 6mm long  $\text{Al}_2\text{O}_3$  crystal along its optical axis. The beam is then collimated by the lens 5 and passes through a second polarizer 6 *parallel* to the first one. A color CCD camera registers the intensity distribution in the computer 8. Typical intensity pattern for the topological quadrupole is shown in Fig. 3(a); we note the excellent agreement with the numerically calculated image in Fig. 1(a). An appropriate choice of the focal length of lens 3 ( $f = 3$  cm) enables us to suppress to a great extent additional vortices located at the periphery of the beam [slightly visible in Figs. 1(a) and 3(a)], so that the beam carries a topological quadrupole only.

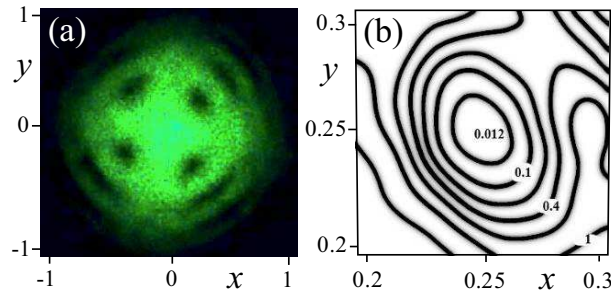


Fig. 3. Experimentally measured (a) intensity distribution of the linearly polarized topological quadrupole and (b) the intensity levels in the vicinity of the single-charge vortex in the right top quadrant of the plot (a).

### 3. Single-charge monochromatic vortex

The structure of each vortex nested in the quadrupole differs from an ideal radially symmetric vortex, as shown in Figs. 1(b) and 3(b). To examine this structure more closely, we note that the field  $E_x$  has a number of phase singularities with azimuthal coordinates  $\varphi = \pm\pi/4, \pm3\pi/4$ , located on rings with radii  $r_p = \sqrt{(2p+1)\pi/a}$ , found from the conditions  $\text{Re} E_x = 0$  and  $\text{Im} E_x = 0$ , here  $a = k\Delta n/l$ ,  $\Delta n \approx n_o\alpha/2$  with  $n_o = 2$ , and  $p = 0, 1, 2, \dots$ . Variation of the beam waist at the plane  $z = 0$  enables us to find the beam pattern at the crystal output such that it corresponds to the beam bearing a single topological quadrupole on the ring with  $r_0^2 = \pi/a$ . The field in the vicinity of an isolated singularity with  $\varphi_0 = \pi/4$  can be written as  $E_x \propto x' + y' - i2(x' - y')/\pi$ , where  $\mathbf{r}' = \mathbf{r} - \mathbf{r}_0$ . The lines of the equal intensity near

the singularity have an elliptical shape with the main axes tilted by  $45^\circ$  (see Figs. 1 and 3),  $|E_x|^2 \propto (x' + y')^2/4 + (x' - y')^2/\pi^2$ , which can be characterized by the degree of ellipticity,  $Q = 2/\pi \propto 0.64$ . The vortex deformation depends neither on the crystal nor the beam parameters, and it represents a geometrical constraint of the crystal-generated beams. From the experimental data shown in Fig. 3(b) we measure a relief of the beam intensity near the vortex core and find the ellipticity  $Q^{\text{exp}} = 0.71$  which is close to the theoretical value of 0.64.

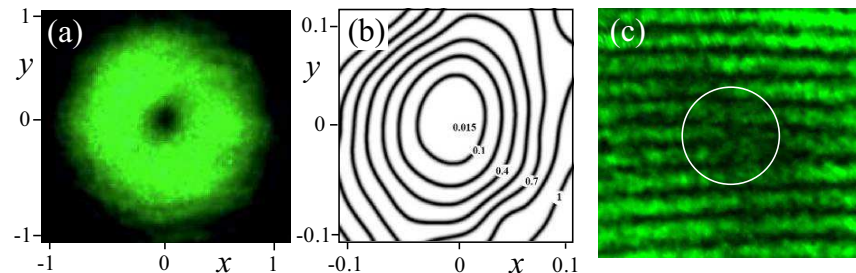


Fig. 4. Experimentally measured (a,b) intensity and (c) interferogram of a single-charge monochromatic vortex generated by the beam tilted with respect to the crystal axis at an angle  $\Theta \approx 1.4^\circ$ . Corresponding movie ([single.avi, 2.4MB](#)) demonstrates the process of the vortex generation as the beam propagates through the crystal.

Furthermore, we demonstrate that a single-charge vortex can be isolated from the quadrupole by propagating the optical beam under a small angle to the optical axis of the crystal,  $\Theta = r_0/l = \sqrt{\pi}/(\Delta nkl)$ . For this angle, the centre of the beam at the output matches the position  $\mathbf{r}_0$  of one of the optical vortices in the quadrupole. The experimental results presented in Fig. 4, show a distinct intensity minimum at the beam axis. Such a minimum does not necessary guarantee the presence of a phase singularity because for a tilted beam the ordinary and extraordinary polarization components propagate in different directions due to birefringence. The phase singularity is confirmed by interference of the output and a plane reference beam. The interferogram [Fig. 4(c)] bears a fork pattern characteristic for a single-charge optical vortex. The numerical simulations (see the movie in Fig. 4) demonstrate that a single-charge optical vortex can be indeed formed at the output facet of the crystal if the inclination angle is properly adjusted for a given crystal length. While the vortex in numerical simulations is strongly deformed, a visual comparison of the vortex in a topological quadrupole in Fig. 3(b) and the isolated vortex in Fig. 4(b) shows that the vortex quality is greatly improved in the later case.

#### 4. Single-charge polychromatic vortex

To generate a polychromatic vortex we employ a partially spatially coherent white-light source. We use an ordinary incandescent 50W lamp with a tungsten filament ( $0.5 \times 2$  mm). The lamp is placed into a spherical reflector 9 (see the inset in Fig. 2). The radiation is directed into a collimator and then projected onto a diffuser of a lusterless glass to blur the image of the filament. The scattered light is then focused by a lens with  $f = 4$  cm into the spatial filter with an inner diaphragm to adjust the degree of spatial coherence of the beam. In our experiments, the diaphragm radius is about 1 mm. The beam divergence behind the spatial filter is about  $15^\circ$  indicating very low spatial coherence. The beam then passes through the polarizer 2, and is focused by the lens 3 with  $f = 3$  cm onto the crystal. The transmitted radiation is collected by the lens 5 and passes through a polarizer into the CCD camera. Figure 5(a) shows an experimental image of the singular beam, which major feature is the rainbow-like distribution of colors near the beam axis. This is in contrast to the earlier reported generation double-charge white vortex

with the origins coinciding for all wavelengths [16, 21]. This phenomenon is explained by a chromatic dispersion of light rays transmitted at some angle to the optical axis [8]. Figure 5(b) shows the transverse intensity profiles for the three basic colors: red (R), green (G), and blue (B), which clearly indicates that the intensity minima for different colors are located at different points. As a result, the vortex core is blurred, and it gains a rainbow coloring.

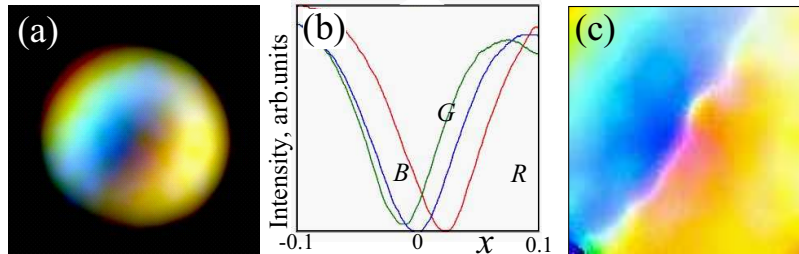


Fig. 5. Spatially strongly incoherent polychromatic vortex beam: (a) intensity, (b) intensity cuts for three main colours, and (c) the chromoscopic vortex image.

The presence of phase singularities is normally detected using interferometric experiments [3, 23, 24]. However, the low spatial coherence of our beam makes such measurements difficult. Therefore, to confirm the presence of a phase singularity, we apply the method suggested by Berry [25]. With this method, we record the RGB image of the polychromatic vortex beam and equalize the tint intensities by applying a colour normalization at each pixel of the image accordingly to the expression  $(R, G, B)^T \Rightarrow (R, G, B)^T / \max(R, G, B)$ . The resulting image, called a 'chromoscopic' image [25], is shown in Fig. 5(c). A white line in the distribution of the colour tints inside a vortex core separates two groups of colours, blue and red; the appearance of this line proves the presence of a polychromatic optical vortex.

## 5. Conclusions

We have suggested and demonstrated a novel experimental technique for generation of mono- and polychromatic single-charge optical vortices by manipulating polarization singularities in birefringent crystals. We first studied the generation of a topological quadrupole by sending a linearly polarized light through an uniaxial crystal along its optical axis. We analyzed the properties of the quadrupole beam and found that its four constituent vortices are elliptically deformed. Tilting the input beam at a specific angle to the crystal optical axis, we generated mono- and polychromatic beams with single-charge optical vortices. The quality of an isolated vortex core is essentially improved in comparison to a local vortex within the topological quadrupole. However, in contrast to the on-axis circularly polarized double-charge white optical vortex [16, 21], the linearly polarized single-charge vortex attains a rainbow colouring due to the chromatic dispersion. The vortex colouring is defined mainly by the spectral properties of the initial beam, and it depends weakly on its spatial coherence.

## Acknowledgements

We thank A. F. Rubass from the Taurida National University (Simferopol, Ukraine) for his help with verifying experiments. A. Volyar is grateful to A. P. Kiselev from the Institute of Mathematics (St. Petersburg, Russia) and M. R. Dennis from University of Southampton (UK) for helpful discussions of related mathematical problems.